Article No. jmbi.1999.3184 available online at http://www.idealibrary.com on IDEAL® J. Mol. Biol. (1999) 293, 449–455

JMB

COMMUNICATION

A 2.6 Å Structure of a Serpin Polymer and Implications for Conformational Disease

James A. Huntington, Navraj S. Pannu, Bart Hazes, Randy J. Read David A. Lomas and Robin W. Carrell*

Division of Structural Medicine, Department of Haematology, University of Cambridge, Cambridge Institute for Medical Research Cambridge, CB2 2XY, UK

*Corresponding author

The function of the serpins as proteinase inhibitors depends on their ability to insert the cleaved reactive centre loop as the fourth strand in the main A β-sheet of the molecule upon proteolytic attack at the reactive centre, P1-P1′. This mechanism is vulnerable to mutations which result in inappropriate intra- or intermolecular loop insertion in the absence of cleavage. Intermolecular loop insertion is known as serpin polymerisation and results in a variety of diseases, most notably liver cirrhosis resulting from mutations of the prototypical serpin α_1-antitrypsin. We present here the 2.6 Å structure of a polymer of α_1-antitrypsin cleaved six residues N-terminal to the reactive centre, P7-P6 (Phe352-Leu353). After self insertion of P14 to P7, intermolecular linkage is affected by insertion of the P6-P3 residues of one molecule into the partially occupied β-sheet A of another. This results in an infinite, linear polymer which propagates in the crystal along a 2-fold screw axis. These findings provide a framework for understanding the uncleaved α_1-antitrypsin polymer and fibrillar and amyloid deposition of proteins seen in other conformational diseases, with the ordered array of polymers in the crystal resulting from slow accretion of the cleaved serpin over the period of a year.

Keywords: serpin; polymer; α_1-antitrypsin; structure; amyloid

Serpins have an inherent metastability necessary for their function as serine proteinase inhibitors. Full reactive centre loop insertion into β-sheet A occurs after cleavage at the P1-P1′ position by the attacking proteinase and results in a significant increase in the stability of the serpin with a destabilisation of the trapped proteinase (Loebermann *et al*., 1984; Wright & Scarsdale, 1995). The complexity of this mechanism allows for tight regulation of the inhibitory activity of the serpin, but it brings with it a vulnerability to inappropriate loop insertion. Large numbers of mutations have now been identified in human serpins (Stein & Carrell, 1995) that decrease their stability and allow for the ready formation of polymers linked by the insertion of the reactive loop of one molecule into the A-sheet of the next (Schulze *et al*., 1990). The best studied examples are the common mutations of the plasma protein α_1-antitrypsin that have been shown to cause emphysema and liver disease (Lomas *et al*., 1992). Polymers taken from diseased livers and also those formed *in vitro* appear on electron micrographs as highly flexible ''beads-on-a-string'', occasionally self terminating by circularising into a ''necklace'' (Lomas *et al*., 1992, 1993; Mast *et al*., 1992). A molecular model for these polymers has been constructed from the native structure of α_1-antitrypsin by inserting a preformed β-strand on the reactive centre loop of one molecule as the fourth strand in the β-sheet A of another (Elliott *et al*., 1996). This model, however, is based on the deduction that serpins are capable of such intermolecular loop insertion, but this has not been demonstrated structurally. Here, we present the 2.6 Å structure of a polymer formed upon cleavage of the reactive centre loop of a recombinant form of the natural Pittsburgh mutant (Owen *et al*., 1983) of α_1-antitrypsin (M358R). Cleavage has taken place six residues prior to the reactive centre (P7-P6), resulting in the intermolecular insertion of the P6-P3 region of one molecule into the corresponding gap in β-sheet A of another (Figure 1(a) and (b)). The structural basis of this polymer was predicted by Mast *et al*. (1992) after demonstration of stable polymer formation

E-mail address of the corresponding author: rwc1000@cus.cam.ac.uk

0022-2836/99/430449–7 $30.00/0

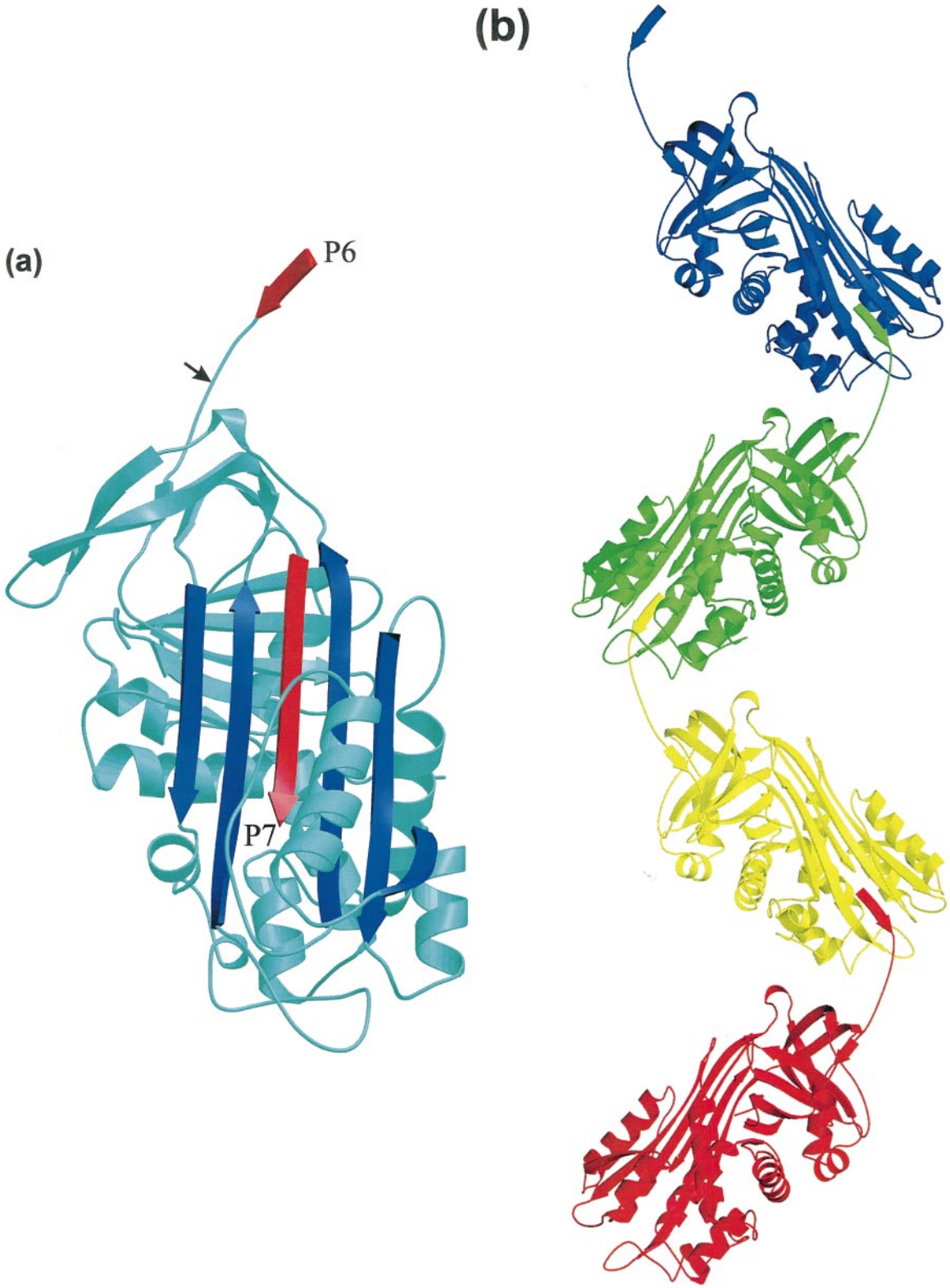

Figure 1 (*legend shown on page 452*)

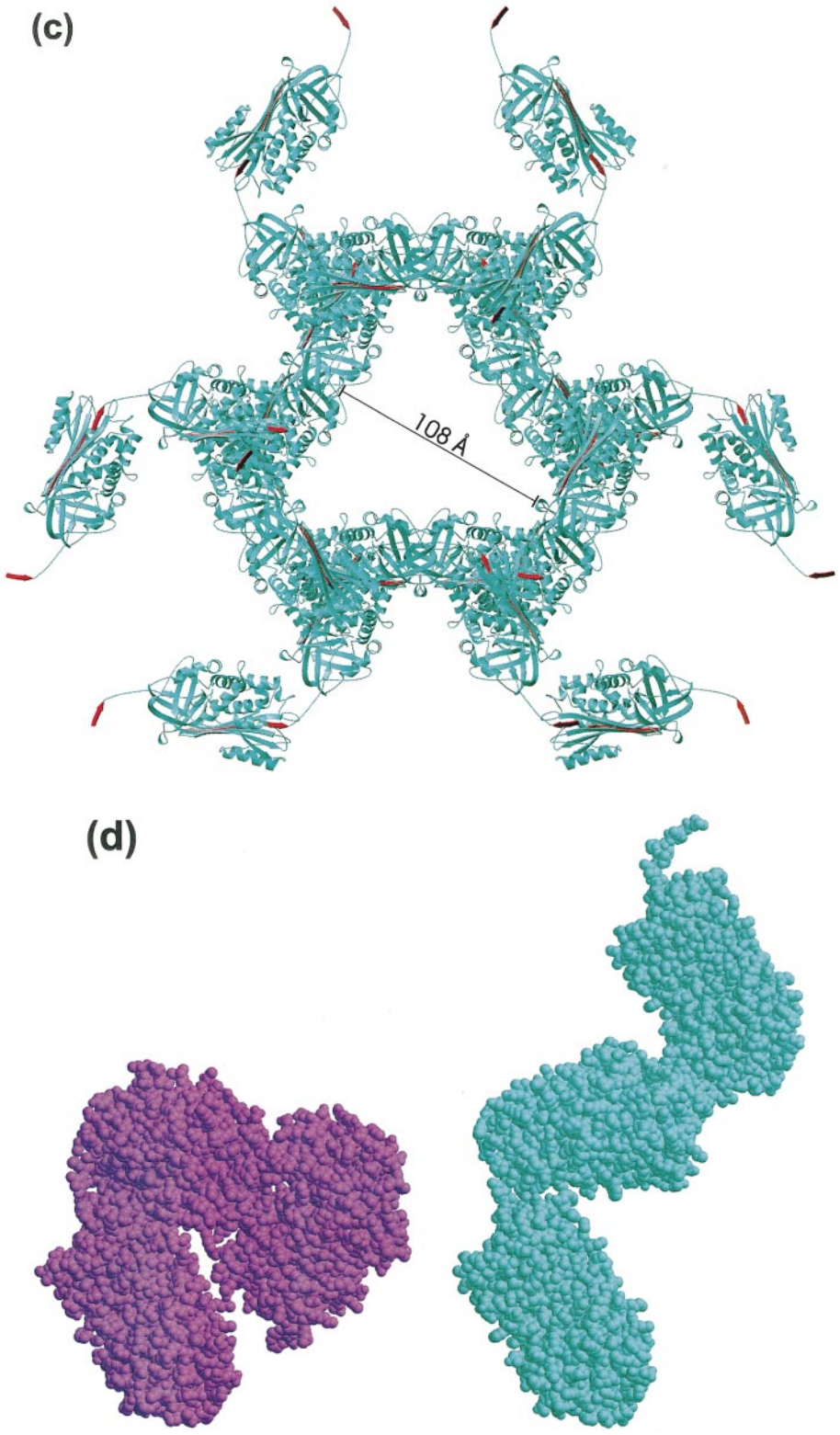

Figure 1 (*legend shown on page 452*)

subsequent to cleavage within the reactive centre loop. The behaviour of this polymer on native PAGE and transverse urea gradient gels, and its appearance on electron micrographs indicates its morphological similarity to that of the uncleaved polymers observed in disease.

Crystals of the polymer were obtained from drops containing recombinant α_1-antitrypsin Pittsburgh and recombinant S195A thrombin which grew over a period of one year at 18 °C. The two proteins form a tight reversible complex which represents the serpin:proteinase Michaelis complex and it was for this purpose that crystallisation trials were set up. The rate of crystal growth was necessarily slow, since the polymer forms as a consequence of the incidental cleavage of the inhibitor. Cleavage was limited to the P7-P6 site (Phe352-Leu353), presumably either as a result of blockage of the P1-P1′ site by the binding of the inactive thrombin or by the nature of the P1 residue which is a Met residue in wild-type α_1-antitrypsin and an Arg residue in the Pittsburgh variant (Owen *et al*., 1983). We do not know which proteinase was involved or which organism produced it, but such incidental cleavage has previously been observed during the crystallisation of wild-type α_1-antitrypsin (Loebermann *et al*., 1984). The cleavage site is of general specificity for chymotrypsin-like serine proteinases and the cysteine proteinase papain (Chang *et al*., 1996). N-terminal sequencing of a single crystal in 0.1 % (w/v) SDS is consistent with only one cleavage site in the reactive centre loop at position P7-P6. The composition of the mother liquor taken from drops containing crystals was determined by N-terminal sequencing and contained a sevenfold excess of thrombin over uncleaved α_1-antitrypsin, with no reactive centre loop cleaved α_1-antitrypsin. The crystals thus provided a sink where cleaved α_1-antitrypsin was deposited directly upon formation, in this way avoiding the formation of free soluble polymer which would have been a detriment to crystal formation.

Table 1 is a summary of the crystallographic statistics. The space group was determined to be $P3_121$ with one molecule per asymmetric unit. The unit cell of the crystal had an unusually high solvent content (73 %). Figure 1(c) shows a 108 Å diameter hole in the crystal lattice when viewed down the 3-fold screw axis. This Figure also illustrates the propagation of the infinite polymer perpendicular to the screw axis. The structure of the cleaved monomer is given in Figure 1(a). The model is essentially unchanged from that of P1-P1′ cleaved α_1-antitrypsin structure (Engh *et al*., 1989). Continuous density is seen of the backbone for the entirety of the model even when the map is contoured at twice the r.m.s. of the map. Figure 2(a) is a stereo representation of the dimer with an omit map generated in the absence of the entire reactive centre loop, P15-P5′, at four times the r.m.s. of the map. Continuous density between the monomers is evident, as is the break between residues Phe at P7 and Leu at P6, demonstrating the site of cleavage (Figure 2(b)).

Electron micrographs of both uncleaved and cleaved polymers indicate similar ability to form tight turns and circular polymers (Lomas *et al*., 1993; Mast *et al*., 1992). However, the current model for the uncleaved polymer (Elliott *et al*., 1996; Mahadeva *et al*., 1999) is compact relative to the structure of the cleaved polymer and it is not apparent how it would allow for sufficient flexibility to give the forms seen on electron micrographs. Figure 1(d) is a space-filling representation of the model of the uncleaved α_1-antitrypsin polymer (magenta) and the structure of the cleaved α_1-antitrypsin polymer (cyan). The structure of the cleaved polymer, with its flexible connecting loops (Figure 1(b)), favours a modification of the original model to allow an increased flexibility and supports other evidence for an extension of the reactive loop. Extension of the intact loop would require the release of strand 1 from the C-sheet at the distal hinge of the loop, since the proximal hinge is fixed at the terminus of strand 5 of the

Figure 1. (a) Monomer of the P7-P6 cleaved Pittsburgh α_1-antitrypsin in the classical view with β-sheet A in blue and the portion of the reactive centre loop which becomes strand 4A after cleavage in red. The normal scissile bond (P1-P1′) is indicated by the arrow. Cleavage at this site results in a full occupancy of β-sheet A with the inclusion of residues P15 through P3 as s4A. The P7 and P6 residues are indicated and are separated by 70 Å. The effect of cleavage at P7-P6 is a partial occupancy of the strand 4A allowing for ready insertion of the residues C-terminal to the cleavage site, P6*-P3*, from another monomer. (b) Such intermolecular loop insertion is demonstrated in the structure of a tetramer extracted from the infinite polymer, with the P6-P3 segment of one monomer clearly visible within the β-sheet A of the other. Insertion is in register with P1-P1′ cleaved α_1-antitrypsin. The monomers which compose the polymer are related in the crystal by a 2_1-fold screw axis parallel to the a cell edge. (c) The view down the 3_1-fold screw axis of the crystal lattice reveals its tube-like nature. The unusually high solvent content of 73 % is explained by the 108 Å diameter hole that extends for the length of the crystal. (d) The current model of the uncleaved α_1-antitrypsin trimer (magenta) (Elliott *et al*., 1996; Mahadeva *et al*., 1999) and the structure of the cleaved α_1-antitrypsin trimer (cyan) in space-filling representation after superposition of the first monomer. Polymerisation for the uncleaved model is affected by in register insertion of the P8 to P3 of the reactive centre loop into the β-sheet A of the following monomer. The model is thus constrained and cannot adopt the conformation of the cleaved polymer with which it is morphologically similar by electron microscopy. The Figures were generated using Molscript (Kraulis, 1991) and Raster3D (Bacon & Anderson, 1988; Merritt & Murphy, 1994).

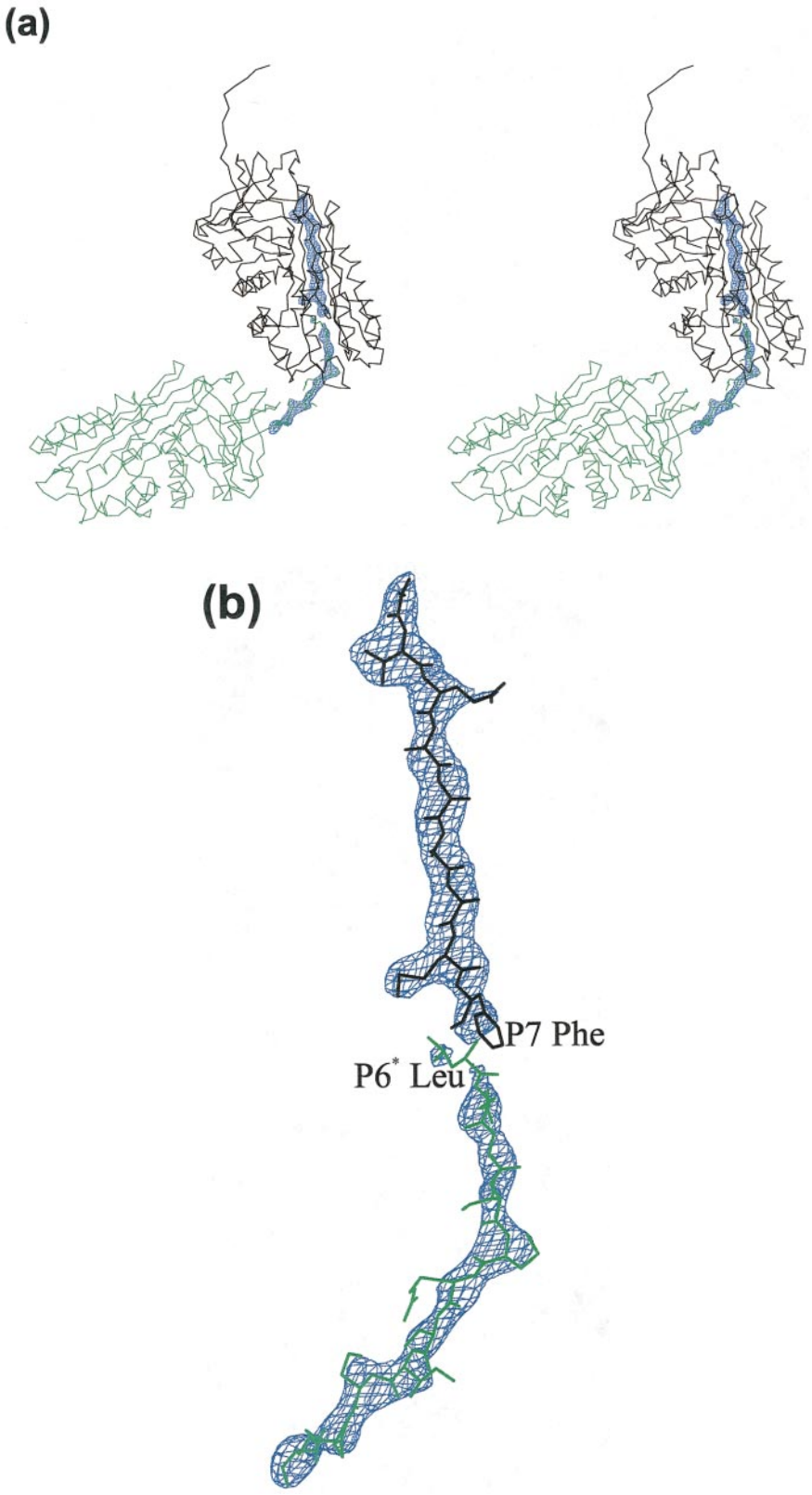

Figure 2. (a) A stereo view of the cleaved α_1-antitrypsin dimer with a σ_A-weighted omit map, contoured at four times the r.m.s. of the map, for the region extending from P15 to P5′, shows the unequivocal nature of the dimer contact. Continuous density is observed for the entire length of strand 4A of the black monomer into strand 1C of the next monomer in green. Weak density is observed at the site of cleavage. (b) A close-up of the omit map at the site of cleavage. P15 to P7 is in black with P6* to P5′* of the dimer partner in green. The omit map was computed after refinement using the model of cleaved α_1-antitrypsin with the reactive centre loop (P15-P5′) removed.

Table 1. Statistics for data collection and refinement

Space group	$P3_121$
Cell constants (Å)	$a=b=108.59$, $c=110.65$
Matthew's coefficient (Å^3 D$_a^{-1}$)	4.46
Resolution range	27.27-2.57 Å
Overall R_{merge} (%)	20.9
$\langle F_o/\sigma(F_o)\rangle$	
Overall	13.73
Highest resolution bin (2.66-2.57 Å)	2.33
Data completeness (%)	
Overall	71.5
Highest resolution bin (2.66-2.57 Å)	12.5
Reflections measured	17,423
Effective resolution[a] (Å)	2.88
Non-hydrogen protein atoms	2873
Water molecules	23
R-factor (%)	21.2
R_{free}[b] (%)	25.8
r.m.s. deviations	
Bond angles (deg.)	1.281
Bond lengths (Å)	0.005

Data were collected from a single frozen crystal at beamline 9.6 at the SRS in Daresbury. Crystal growth conditions, 30% (w/v) PEG400, 200 mM NaCl, 100 mM Tris (pH 8.5), provided adequate cryoprotection. The data were processed using MOSFLM (Leslie, 1992) and merged using SCALA from the CCP4 package (CCP4, 1994). Data extended to 2.57 Å resolution with an overall completeness of 71.5% and an overall R_{merge} of 20.9%. The structure was solved by molecular replacement in AMoRe (Navaza, 1994) using cleaved α_1-antitrypsin with its reactive centre loop removed as a search model (Engh *et al.*, 1989). The absence of thrombin was verified by the absence of a molecular replacement solution and the quality of the agreement using cleaved α_1-antitrypsin alone. Rigid body refinement of this solution in CNS (Brünger *et al.*, 1998) led to an R_{free} of 35.2% and an *R*-factor of 33.2% for data between 27.3 and 3.0 Å. An iterative procedure of model building using the XtalView package (McRee, 1992) with a model including a correction for bulk solvent (Jiang & Brünger, 1994) with cross-validated SigmaA-weighted maps (Read, 1997) and refinement in CNS using a maximum likelihood target (Pannu & Read, 1996) yielded the final R_{free} and *R*-factor of 25.8% and 21.2%, respectively, for all data between 27.3 and 2.57 Å.

[a] Resolution of a hypothetical 100% complete data set containing 17,423 reflections, calculated in SFTOOLS (B.H., unpublished results).

[b] The R_{free} set consisted of 875 reflections, selected randomly.

A-sheet. Such s1C release has been previously observed in serpins in the fully self-loop-inserted latent conformation (Mottonen *et al.*, 1992). Furthermore, although loop-sheet polymerisation is known to result from mutations that destabilise the A-sheet, it has also been observed as an unexplained consequence of mutations that perturb the stability of s1C. Moreover, support for the hypothesis of s1C release upon polymer formation comes from the demonstration that the immobilisation of s1C by disulphide bridging prevents polymerisation (Chang *et al.*, 1997). In the past, the interpretation of these diverse results has been complicated by uncertainty as to whether the pathological polymerisation of the serpins resulted from A or C-sheet insertion of the reactive centre loop. The body of evidence now clearly indicates A-sheet linkage, together with the conclusion that this also requires a concomitant release of strand 1 from the C-sheet.

The mechanism of loop-sheet polymerisation is of direct relevance to a range of diseases resulting from dysfunctions of the serpins including thrombosis and immune hypersensitivity, as well as emphysema and cirrhosis (Stein & Carrell, 1995). However, of even wider interest is the model that the serpins are now providing for the general mechanisms that result in conformational diseases (Carrell & Lomas, 1997). In particular, the results described here are relevant to the changes that lead to β-amyloid deposition in Alzheimer's disease. As with the formation of the polymers, the release of the Alzheimer's Aβ42 peptide results from an initial irregularity of proteinase cleavage followed by β-strand linkage with the formation of protofibrils at very low concentrations. The formation of plaques is believed to result from subsequent nucleation-dependent polymerisation (Lansbury, 1999; Harper & Lansbury, 1997). Although the α_1-antitrypsin polymers shown here are linked by small-scale domain swapping (Bennett *et al.*, 1994), it is also known that unrelated peptides can readily insert into the A-sheet (Chang *et al.*, 1996; Xue *et al.*, 1998). This gives relevance to the observation that a related serpin, α_1-antichymotrypsin, is consistently present in the amyloid plaques of Alzheimer's disease (Abraham *et al.*, 1988) and has been shown to interact *in vitro* with the Aβ42 peptide and thereby nucleate protofibril formation (Ma *et al.*, 1994).

Protein Data Bank number

Coordinates have been deposited in the Protein Data Bank (accession number 18mb).

Acknowledgements

We thank Charles T. Esmon for providing the inactive thrombin. This work was supported by the Wellcome Trust (R.W.C., 039046; R.J.R. 050211) and by the NIH (J.A.H. HL09927). N.S.P. is supported by Wellcome Trust and NSERC studentships.

References

Abraham, C. R., Selkoe, D. J. & Potter, H. (1988). Immunochemical identification of the serine protease inhibitor α_1-antichymotrypsin in the brain amyloid deposits of Alzheimer's disease. *Cell,* **52**, 487-501.

Bacon, D. & Anderson, W. F. (1988). A fast algorithm for rendering space-filling molecule pictures. *J. Mol. Graph.* **6**, 219-220.

Bennett, M. J., Choe, S. & Eisenberg, D. (1994). Domain swapping: entangling alliances between proteins. *Proc. Natl Acad. Sci. USA,* **91**, 3127-3131.

Brünger, A. T., Adams, P. D., Clore, G. M., Delano, W. L., Gros, P., Grosse-Kunstleve, R. W., Jiang, J. S., Kuszewski, J., Nilges, M., Pannu, N. S., Read, R. J.,

Rice, L. M., Simonson, T. & Warren, G. L. (1998). Crystallography & NMR system: a new software suite for macromolecular structure determination. *Acta Crystallog. sect. D,* **54**, 905-921.

Carrell, R. W. & Lomas, D. A. (1997). Conformational disease. *Lancet,* **350**, 134-138.

Chang, W. S., Wardell, M. R., Lomas, D. A. & Carrell, R. W. (1996). Probing serpin reactive-loop conformations by proteolytic cleavage. *Biochem. J.* **314**, 647-653.

Chang, W. S., Whisstock, J., Hopkins, P. C., Lesk, A. M., Carrell, R. W. & Wardell, M. R. (1997). Importance of the release of strand 1C to the polymerization mechanism of inhibitory serpins. *Protein Sci.* **6**, 89-98.

Collaborative Computational Project Number 4 (1994). The CCP4 suite: programs for protein crystallography. *Acta Crystallog. sect. D,* **50**, 760-763.

Elliott, P. R., Lomas, D. A., Carrell, R. W. & Abrahams, J. P. (1996). Inhibitory conformation of the reactive loop of α_1-antitrypsin. *Nature Struct. Biol.* **3**, 676-681.

Engh, R., Lobermann, H., Schneider, M., Wiegand, G., Huber, R. & Laurell, C. B. (1989). The S variant of human α_1-antitrypsin, structure and implications for function and metabolism. *Protein Eng.* **2**, 407-415.

Harper, J. D. & Lansbury, P. T. J. (1997). Models of amyloid seeding in Alzheimer's disease and scrapie: mechanistic truths and physiological consequences of the time-dependent solubility of amyloid proteins. *Annu. Rev. Biochem.* **66**, 385-407.

Jiang, J. S. & Brünger, A. T. (1994). Protein hydration observed by X-ray diffraction. Solvation properties of penicillopepsin and neuraminidase crystal structures. *J. Mol. Biol.* **243**, 100-115.

Kraulis, P. J. (1991). Molscript - a program to produce both detailed and schematic plots of protein structures. *J. Appl. Crystallog.* **24**, 946-950.

Lansbury, P. T. J. (1999). Evolution of amyloid: what normal protein folding may tell us about fibrillogenesis and disease. *Proc. Natl Acad. Sci. USA,* **96**, 3342-3344.

Leslie, A. W. G. (1992). *Joint CCP4 and ESF-EACMB Newsletter on Protein Crystallography*, vol. 26, Daresbury Laboratory, Warrington, UK.

Loebermann, H., Tokuoka, R., Deisenhofer, J. & Huber, R. (1984). Human α_1-proteinase inhibitor. Crystal structure analysis of two crystal modifications, molecular model and preliminary analysis of the implications for function. *J. Mol. Biol.* **177**, 531-557.

Lomas, D. A., Evans, D. L., Finch, J. T. & Carrell, R. W. (1992). The mechanism of Z α_1-antitrypsin accumulation in the liver. *Nature,* **357**, 605-607.

Lomas, D. A., Finch, J. T., Seyama, K., Nukiwa, T. & Carrell, R. W. (1993). α_1-Antitrypsin Siiyama (Ser53 $\rightarrow$ Phe). Further evidence for intracellular loop-sheet polymerization. *J. Biol. Chem.* **268**, 15333-15335.

Ma, J., Yee, A., Brewer, H. B. J., Das, S. & Potter, H. (1994). Amyloid-associated proteins α_1-antichymotrypsin and apolipoprotein E promote assembly of Alzheimer β-protein into filaments. *Nature,* **372**, 92-94.

Mahadeva, R., Chang, W. S., Dafforn, T. R., Oakley, D. J., Foreman, R. C., Calvin, J., Wight, D. G. & Lomas, D. A. (1999). Heteropolymerization of S, I, and Z α_1-antitrypsin and liver cirrhosis. *J. Clin. Invest.* **103**, 999-1006.

Mast, A. E., Enghild, J. J. & Salvesen, G. (1992). Conformation of the reactive site loop of α_1-proteinase inhibitor probed by limited proteolysis. *Biochemistry,* **31**, 2720-2728.

McRee, D. E. (1992). A visual protein crystallographic software system for X11/XView. *J. Mol. Graph.* **10**, 44-46.

Merritt, E. A. & Murphy, M. E. P. (1994). Raster3d version-2.0 - a program for photorealistic molecular graphics. *Acta Crystallog. sect. D,* **50**, 869-873.

Mottonen, J., Strand, A., Symersky, J., Sweet, R. M., Danley, D. E., Geoghegan, K. F., Gerard, R. D. & Goldsmith, E. J. (1992). Structural basis of latency in plasminogen activator inhibitor-1. *Nature,* **355**, 270-273.

Navaza, J. (1994). AMoRe - an automated package for molecular replacement. *Acta Crystallog. sect. A,* **50**, 157-163.

Owen, M. C., Brennan, S. O., Lewis, J. H. & Carrell, R. W. (1983). Mutation of antitrypsin to antithrombin. α_1-Antitrypsin Pittsburgh (Met 358 Arg), leads to a fatal bleeding disorder. *New Engl. J. Med.* **309**, 694-698.

Pannu, N. S. & Read, R. J. (1996). Improved structure refinement through maximum likelihood. *Acta Crystallog. sect. A,* **52**, 659-668.

Read, R. J. (1997). Model phases: probabilities and bias. *Methods Enzymol.* **277**, 110-128.

Schulze, A. J., Baumann, U., Knof, S., Jaeger, E., Huber, R. & Laurell, C. B. (1990). Structural transition of α_1-antitrypsin by a peptide sequentially similar to β-strand s4A. *Eur. J. Biochem.* **194**, 51-56.

Stein, P. E. & Carrell, R. W. (1995). What do dysfunctional serpins tell us about molecular mobility and disease?. *Nature Struct. Biol.* **2**, 96-113.

Wright, H. T. & Scarsdale, J. N. (1995). Structural basis for serpin inhibitor activity. *Proteins: Struct. Funct. Genet.* **22**, 210-225.

Xue, Y., Bjorquist, P., Inghardt, T., Linschoten, M., Musil, D., Sjolin, L. & Deinum, J. (1998). Interfering with the inhibitory mechanism of serpins: crystal structure of a complex formed between cleaved plasminogen activator inhibitor type 1 and a reactive-centre loop peptide. *Structure,* **6**, 627-636.

Edited by R. Huber

(Received 7 July 1999; received in revised form 8 September 1999; accepted 10 September 1999)